Magn Reson Med Sci, Vol. 14, No. 3, pp. 193–202, 2015 doi:10.2463/mrms.2014-0048

MAJOR PAPER

The Impact of Flip Angle and TR on the Enhancement Ratio of Dynamic Gadobutrol-enhanced MR Imaging: *In Vivo* VX2 Tumor Model and Computer Simulation

Po-Chou Chen[1], Ding-Jie Lin[1], Jo-Chi Jao[2]*, Chia-Chi Hsiao[3], Li-Min Lin[4,5], and Huay-Ben Pan[3]

[1]*Department of Biomedical Engineering, I-SHOU University Kaohsiung 824, Taiwan, ROC*
[2]*Department of Medical Imaging and Radiological Sciences, Kaohsiung Medical University*
[3]*Department of Radiology, Kaohsiung Veterans General Hospital*
[4]*Department of Dentistry, Division of Oral Pathology, Kaohsiung Medical University Hospital*
[5]*School of Dentistry, College of Dental Medicine, Kaohsiung Medical University*
(Received April 18, 2014; Accepted December 10, 2014; published online March 31, 2015)

Dynamic contrast-enhanced magnetic resonance imaging (DCE-MRI) is widely used to diagnose cancer and monitor therapy. The maximum enhancement ratio (ER_{max}) obtained from the curve of signal intensity over time could be a biomarker to distinguish cancer from normal tissue or benign tumors. We evaluated the impact of flip angle (FA) and repetition time (TR) on the ER_{max} values of dynamic gadobutrol-enhanced MR imaging, obtaining T_1-weighted (T_1W) MR imaging of VX2 tumors using 2-dimensional fast spoiled gradient echo (2D FSPGR) with various FAs (30°, 60° and 90°) at 1.5 tesla before and after injection of 0.1 mmol/kg gadobutrol. *In vivo* study indicated significant differences between ER_{max} values and area under the ER-time curve (AUC_{100}) of VX2 tumors and muscle tissue, with the highest ER_{max} and AUC_{100} at FA 90°. Computer simulation also demonstrated the ER as a strictly increasing monotonic function in the closed interval [0°, 90°] for a given TR when using T_1W FSPGR, and the highest ER value always occurred at FA 90°. The FA for the highest ER differed from that for the highest signal-to-noise or contrast-to-noise ratio. For long TR, the ER value increases gradually. However, for short TR, the ER value increases rapidly and plateaus so that the ER value changes little beyond a certain FA value. Therefore, we suggest use of a higher FA, near 90°, to obtain a higher ER_{max} for long TR in 2D SPGR or FSPGR and a smaller FA, much less than 90°, to reach an appropriate ER_{max} for short TR in 3D SPGR or FSPGR. This information could be helpful in setting the optimal parameters for DCE-MRI.

Keywords: ***fast spoiled gradient echo*, *flip angle*, *gadobutrol*, *repetition time*, *VX2 animal model***

Introduction

Cancer incidence increases yearly, and early treatment based on early accurate diagnosis is very important. Dynamic contrast-enhanced magnetic resonance imaging (DCE-MRI) has been used to detect lesions and monitor treatment. Administration of a contrast agent (CA) enables differentiation of enhancement patterns of tumors from those of normal tissues.[1–5]

Gadolinium-diethylenetriamine penta-acetic acid (Gd-DTPA; Magnevist, Schering, Berlin, Germany) is the first CA approved by the U.S. Food and Drug Administration (FDA) since 1988 as a non-specific extracellular CA and has been widely used in DCE-MRI.[6,7] Since then, several novel CAs have also been approved for clinical use. Gadobutrol

*Corresponding author, Phone: +886-7-3121101 ext. 2356-14, Fax: +886-7-3113449, E-mail: jochja@kmu.edu.tw

(Gadovist, Schering, Berlin, Germany) is a neutral, hydrophilic, and macrocyclic contrast agent that has become clinically available. Its higher relaxivities compared to that of Gd-DTPA allows greater contrast between tumor and tissue.[8–11]

The enhancement ratio (ER), calculated from the MR signal intensity after injection of CA divided by that before CA injection, can be a biomarker to distinguish cancers from normal tissue. The relative maximum ER (ER_{max}) can also differentiate malignant from benign masses in some tumors.[12,13] ER_{max} varies with pulse sequence in addition to magnetic field, category of CA, injection dosage of CA, and time interval after injection of CA.[10,14] A T_1-weighted (T_1W) spoiled gradient echo (SPGR) pulse sequence is most commonly used in DCE-MRI, and its signal intensity depends on such scanning parameters as flip angle (FA), repetition time (TR), proton density, and echo time (TE). We investigated the impact of FA and TR on the ER of dynamic gadobutrol-enhanced MR imaging.

VX2 tumors are hypervascular adenocarcinomas often used as a model for human disease and can be implanted in many organs for preclinical studies. In this study, we implanted VX2 tumor cells into one thigh of each of 18 New Zealand rabbits for imaging the thigh and there were no obvious motion artifacts during DCE-MRI.[15–17] We used the rabbit VX2 tumor to compare ER_{max} values obtained using T_1W FSPGR with various FAs. In addition, we examined the effects of FA and TR on the ER values by computer simulation and explored the theoretical approach of optimal FA for the highest ER.

Materials and Methods

MR imaging of animals

Our institutional animal care and use committee approved the protocol for animal use.

We divided 18 rabbits into 3 groups of 6 animals each that were subjected to MR imaging using flip angles of 30°, 60°, or 90°. Each rabbit was implanted with VX2 tumor cells in a concentration of about 1×10^6/mL that was injected intramuscularly into its left thigh using a 0.5 mL VX2 tumor cell suspension via a 19-gauge needle. The injected site was shaved and disinfected with ethanol and povidone iodine. The cell suspension was prepared from a mass removed from a rabbit carrying a VX2 tumor and placed in a cell culture dish with normal saline. The tumor mass was washed 3 times, chopped into very small pieces, and digested with trypsin to form cell suspension.

Two weeks after tumor implantation, the rabbits underwent MR examinations after being anesthetized with 16 mg/kg Zoletil 50 (VIRBAC Animal Health, Carros, France) and 14 mg/kg Rompun 2% (Bayer Korea Ltd., Kyonggi-do, Korea) and inserted a 23-gauge butterfly needle into an ear vein for gadobutrol injection. All MR imaging studies were performed on a 1.5-tesla whole-body MR scanner (Signa HDxt, GE Medical Systems, Milwaukee, WI, USA) with an 8-channel knee coil. The rabbit's left thigh was placed into a knee coil with the VX2 mass in the center.

A phantom of 2% agarose and a phantom of water were put aside the thigh for references. A 3-plane localizer scan was followed by a conventional spin echo (CSE) pulse sequence for T_1 and T_2 measurement and a 2-dimensional (2D) FSPGR pulse sequence for DCE-MRI. The scanning parameters for T_1 measurement were: field of view (FOV), $16 \times 16\ cm^2$; matrix size (MS), 256×128; slice thickness (ST), 5 mm; number of slices (NS), 8; bandwidth (BW), 15 kHz; number of excitations (NEX), one; TE, 14 ms; and TR, 270, 500, 1000, and 2000 ms. T_2 measurement employed the same FOV, MS, ST, BW and NEX as those for T_1 measurement but different TR (2000 ms) and TEs (15, 30, 45 and 60 ms). The scanning parameters for DCE-MRI for each group were: TR, 100 ms; TE, 1.3 ms; BW, 31.3 kHz; and FA, 30°, 60°, or 90°. The scan time for each image was 14 s.

Following acquisition of 4 precontrast images, each rabbit was administered 0.1 mmol/kg gadobutrol by bolus injection through the ear vein that was flushed with one mL of saline. Scans were subsequently performed continuously for 3 min, after which consecutive scans were performed with one scan per minute. The total scan time for DCE-MRI was 30 min. All acquired MR images were transferred to an Advantage Window workstation for analysis.

For data analysis, several regions of interest (ROIs) were chosen from the rims of tumors, muscle, phantom, and background. Angiogenesis at the periphery of tumors resulted in stronger enhancement of the rims than cores of the tumors, and accumulation of more gadobutrol in the rims of tumors enhanced the MR signal. The ROIs from the rims of tumors were selected according to the regions most enhanced in the second DCE images after injection of gadobutrol.

The T_1 and T_2 values of tumor and muscle were obtained by least squares fitting to the values of ROIs of tumor and muscle according to Eqs. [1] and [2] respectively using commercial software (Sigmaplot, version 9.01, Systat Software, San Jose, CA, USA.[18]

$$S = M(1 - 2e^{-(TR-0.5TE)/T_1} + e^{-TR/T_1}), \quad [1]$$

and

$$S = Me^{-TE/T_2}, \quad [2]$$

where S is the MR signal intensity and M is a constant. Because the spin echo signal can be expressed as[18]:

$$S = M_0(1 - 2e^{-(TR-0.5TE)/T_1} + e^{-TR/T_1})e^{-TE/T_2}, \quad [3]$$

where M_0 is magnetization combined with the electric gain, and M_0 can be determined by dividing M by e^{-TE/T_2} according to Eqs. [1] and [3] once T_1 and T_2 are obtained. Afterwards, we obtained the average T_1, T_2, and M_0 of tumor and muscle of the 18 rabbits and used the data for computer simulation.

The ER value was calculated according to Eq. [4]:

$$ER = \frac{S_{post}}{S_{pre}}, \quad [4]$$

where S_{pre} and S_{post} are the MR signal intensity normalized with the 2% agarose phantom and obtained before (S_{pre}) and after (S_{post}) gadobutrol injection. We averaged the signal intensities from 4 MR images obtained before gadobutrol injection to determine the MR signal intensity before gadobutrol injection.

We could obtain the ER-time curve for each ROI and determine the ER_{max} for each ER-time curve. The area under the curve of each ER-time curve (AUC_{100}) was calculated according to Eq. [5]:

$$AUC_{100} = \sum_{n=1}^{j}\left(\frac{1}{2}\right) \times (t_n - t_{n-1}) \times (ER_n + ER_{n-1}), \quad [5]$$

where $\{t_n\}$ was the time series of dynamic scans, t_n was the nth term and ER_n was the ER obtained at t_n after gadobutrol injection. ER_0 was obtained before gadobutrol injection at $t_0 = 0$ s and was equal to one. AUC_{100} was obtained by summing every trapezoid area under the ER-time curve from 0 to 100 s (j = 6).

We used nonparametric Wilcoxon test for the statistical analysis of T_1, T_2, ER_{max}, and AUC_{100} between the tumor and muscle; $P < 0.05$ was considered to represent significant difference. We used nonparametric Kruskal-Wallis test to compare ER values obtained from each of the 3 groups (scanned with FA of 30°, 60°, or 90°). There was a significant difference in the ER_{max} or AUC_{100} among these 3 groups if $P < 0.05$.

After acquisition of the ER, we calculated the concentration, C, of gadobutrol according to Eq. [6]:

$$C = \frac{-1}{r_1 TR}\ln\frac{1 - B \cdot ER}{1 - B \cdot ER\cos(FA)} - \frac{1}{r_1 T_{10}}, \quad [6]$$

where $B = \frac{(1 - e^{-TR/T_{10}})}{(1 - \cos(FA)e^{-TR/T_{10}})}$ and the r_1 value is $4.7\,mM^{-1}s^{-1}$.[19] Then, we determined the average maximum concentrations of tumor (C_{max_t}) and muscle (C_{max_m}) of the 18 rabbits. The average noise (σ) of the DCE-MRI was obtained by averaging the standard deviation of background signal measured from the 18 rabbits. C_{max_t}, C_{max_m}, and σ were used for computer simulation.

After experiments were completed, rabbits were sacrificed under deep anesthesia with CO_2. The left thigh with implanted VX2 tumor was then removed and fixed in 10% formalin. Paraffin-embedded sections were stained with hematoxylin and eosin for visualization of VX2 tumors under a microscope.

Computer simulation

The signal-to-noise ratio (SNR), ER, and contrast-to-noise ratio (CNR) values for SPGR were calculated according to Eqs. [7] through [10][20,21]:

$$S = M_0\left[\frac{\sin(FA)(1 - e^{-TR/T_1})}{(1 - \cos(FA)e^{-TR/T_1})}e^{-TE/T_2^*}\right], \quad [7]$$

$$SNR = S/\sigma, \quad [8]$$

$$ER = \left[\frac{\sin(FA)(1 - e^{-TR/T_1})}{(1 - \cos(FA)e^{-TR/T_1})}e^{-TE/T_2^*}\right] \Big/ \left[\frac{\sin(FA)(1 - e^{-TR/T_{10}})}{(1 - \cos(FA)e^{-TR/T_{10}})}e^{-TE/T_{20}^*}\right], \quad [9]$$

and

$$CNR = SNR_t - SNR_m, \quad [10]$$

where SNR_t is the SNR of tumor, and SNR_m, that of muscle.

Here, the M_0, T_{10}, T_{20} of tumor and muscle and σ were determined from the MR imaging study mentioned above. Ignoring the impact of field inhomogeneity, we assumed $T_2^* = T_2$.[22] The T_1 and T_2 values of tumor and muscle after gadobutrol injection were calculated according to Eqs. [11] and [12][23]:

$$\frac{1}{T_1} = \frac{1}{T_{10}} + r_1 C, \quad [11]$$

and

$$\frac{1}{T_2} = \frac{1}{T_{20}} + r_2 C, \quad [12]$$

where C is the concentration of the contrast agent, r_1 is longitudinal relaxivity, r_2 is transverse relax-

ivity, T_1 is the longitudinal relaxation time and T_2, the transverse relaxation time after CA injection, and T_{10} is the longitudinal relaxation time and T_{20}, the transverse relaxation time in the absence of CA.

Concentrations C_{max_t} and C_{max_m} were also obtained from the *in vivo* MR imaging studies mentioned above. In the calculation, we used the value 4.7 $mM^{-1}s^{-1}$ for r_1 and 6.8 $mM^{-1}s^{-1}$ for r_2.[19] We evaluated the SNR, ER, and CNR values of tumor and muscle for various FAs (one to 90°) and TRs (5 to 100 ms) with concentrations of C_{max_t} and C_{max_m} and those of tumor with 0.5 mM gadobutrol concentration.

Results

MR imaging of animals

Figure 1 shows CSE images for T_1 measurements and Fig. 2, those for T_2 measurements of tumor and muscle. MR signal intensity increased with TR for a given TE and decreased with TE for a given TR. There were 2 phantoms; one was water and the other was 2% agarose. The water phantom was used to double-check whether the water content in the agarose phantom evaporated. The different inherent proton density and relaxation times of these 2 phantoms yielded different MR signal intensities. In particular, the SNR of water was higher than that of 2% agarose (Fig. 2), which was expected because of the higher proton density and T_2 relaxation time of water. The T_{10} values of tumor were 1812 ± 257 ms and of muscle, 1517 ± 133 ms. The T_{20} values of tumor were 59.17 ± 8.43 ms and of muscle, 31.37 ± 3.43 ms. There were significant differences of T_{10} and T_{20} values between tumor and muscle ($P < 0.01$). The average value of M_0 for tumor was 7456 and for muscle, 5352.

Figure 3 shows several representative dynamic gadobutrol-enhanced MR images from one rabbit. The contrast between tumor and muscle was low before gadobutrol injection. Right after the bolus injection of gadobutrol, the MR signal intensity of the tumor increased more than that of muscle, and consequently, the contrast between tumor and muscle increased. The contrast increased with time, reached a maximum value, and gradually decreased with time as a result of the excretion of gadobutrol. Figure 4a shows the ER-time curves of tumor and muscle obtained with FA/TR/TE = 90°/100 ms/1.3 ms using an FSPGR pulse sequence. The ER of the tumor was higher than that of muscle. Figure 4b shows the ER values of tumor obtained from the same TR/TE (100 ms/1.3 ms), but with various FA (30°, 60°, and 90°). The ER_{max} obtained with a 90° FA was larger than that obtained with FAs of 60° or 30°. Table lists the ER_{max} and AUC_{100} values obtained with various FAs. ER_{max} and AUC_{100} values in the tumor differed significantly from these values in the muscle among the 3 groups scanned with various FAs ($P < 0.05$).

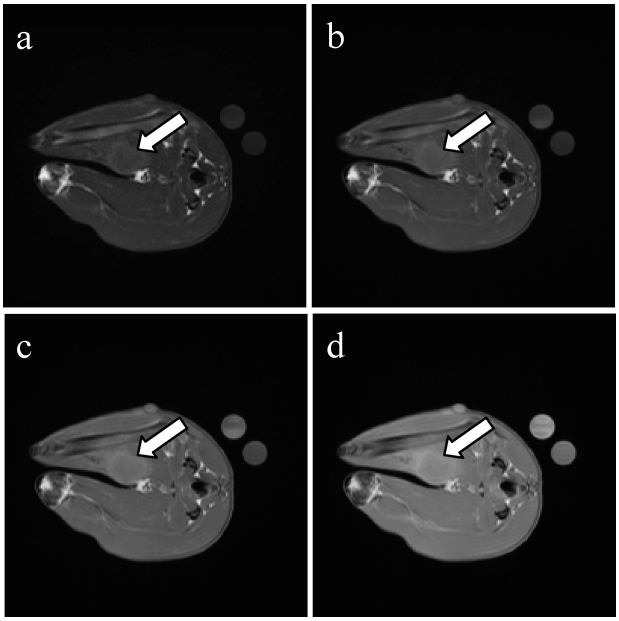

Fig. 1. Conventional spin echo (CSE) magnetic resonance (MR) images of a rabbit thigh with VX2 tumor (arrows) obtained with echo time (TE) of 14 ms and repetition times (TR) of (**a**) 270, (**b**) 500, (**c**) 1000, and (**d**) 2000 ms for the T_1 measurement.

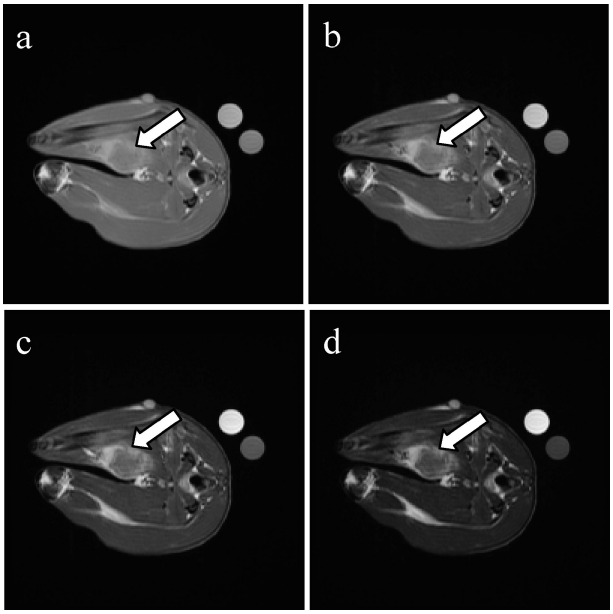

Fig. 2. Conventional spin echo (CSE) magnetic resonance (MR) images of a rabbit thigh with VX2 tumor (arrows) obtained with repetition time (TR) of 2000 ms and echo times (TE) of (**a**) 15, (**b**) 30, (**c**) 45, and (**d**) 60 ms for the T_2 measurement.

The noise value, σ, was 17.57; the C_{max_t} was 0.13 ± 0.04 mM; and the C_{max_m} was 0.03 ± 0.01 mM. The VX2 tumor was verified by hematoxylin and eosin staining (Fig. 5).

Computer simulation

Figure 6 shows SNR values of tumor and muscle as a function of TR and FA. The SNR of tumor was higher than that of muscle for any TR and FA, and the concentration of gadobutrol was 0.13 mM in tumor and 0.03 mM in muscle. The SNR increased with TR for a given FA for both tumor and muscle. However, SNR values increased with FA first and then decreased for some given TR. There was an optimal FA for the maximum SNR (SNR_{max}), and the optimal FA increased with TR as well. Tumor also had higher ER than muscle for each corresponding TR and FA (Fig. 7). The ER values decreased with TR but increased with FA for both tumor and muscle. Figure 9a shows the CNR values as a function of TR and FA. CNR first increased with FA and then decreased for a given TR. The optimal FA was basically defined as that corresponding to the maximum value of SNR, CNR, and ER for each TR (Figs. 7–9). There was an op-

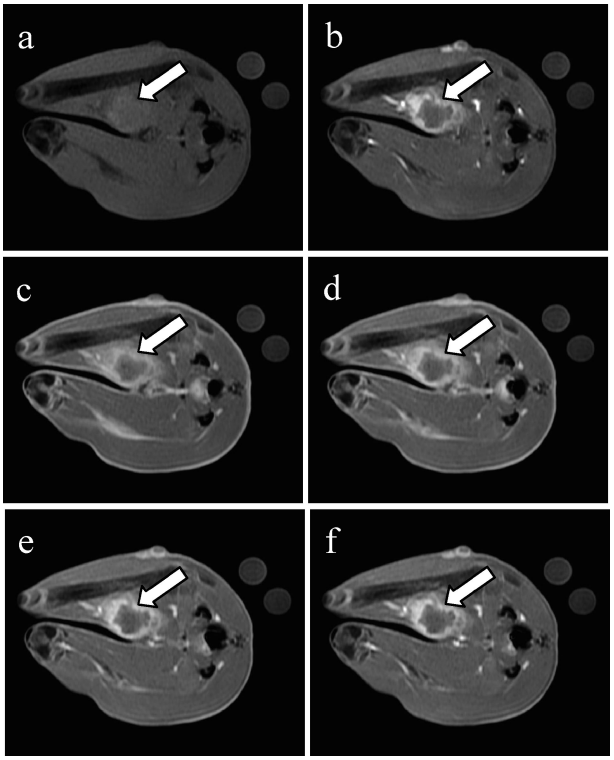

Fig. 3. Dynamic gadobutrol-enhanced images of a rabbit thigh with VX2 tumor (arrows) obtained (**a**) before, (**b**) 14 s, and (**c**) one, (**d**) 3, (**e**) 10, and (**f**) 30 min after gadobutrol injection with 90° flip angle (FA), repetition time (TR) of 100 ms, and echo time (TE) of 1.3 ms.

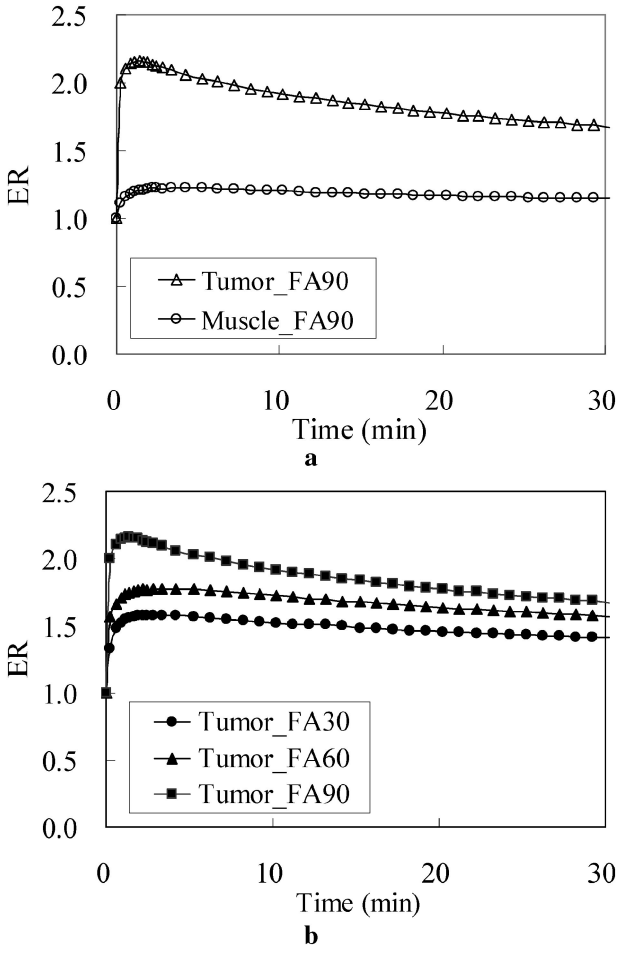

Fig. 4. Enhancement ratio (ER)-time curves of dynamic contrast-enhanced magnetic resonance imaging (DCE-MRI) from (**a**) tumor and muscle with 90 ° flip angle (FA) and (**b**) tumor with variable FAs using fast spoiled gradient echo (FSPGR) pulse sequences (repetition time [TR]/echo time [TE], 100/1.3 ms).

Table. Maximum enhancement ratio (ER_{max}) and area under the ER-time curve (AUC_{100}) with various flip angles (FA)

	Tumor			Muscle		
	FA 30°	FA 60°	FA 90°	FA 30°	FA 60°	FA 90°
ER_{max}	1.60 ± 0.13	1.81 ± 0.20	2.22 ± 0.31	1.16 ± 0.07	1.23 ± 0.04	1.24 ± 0.05
AUC_{100}	142.1 ± 10.5	158.6 ± 18.4	198.2 ± 24.4	107.1 ± 3.2	109.9 ± 3.5	111.1 ± 3.1

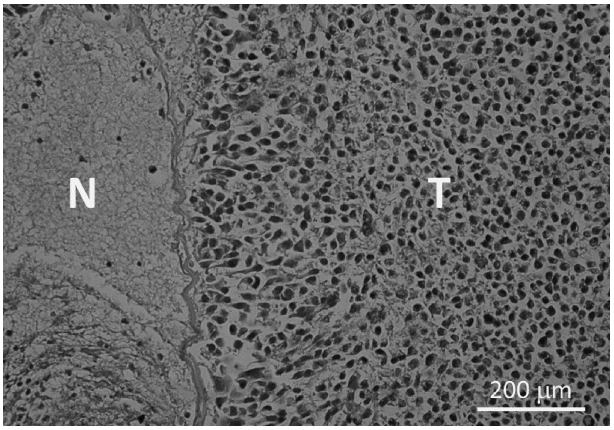

Fig. 5. Microscopic image of VX2 cells. T, VX2 tumor cells; N, normal muscle cells.

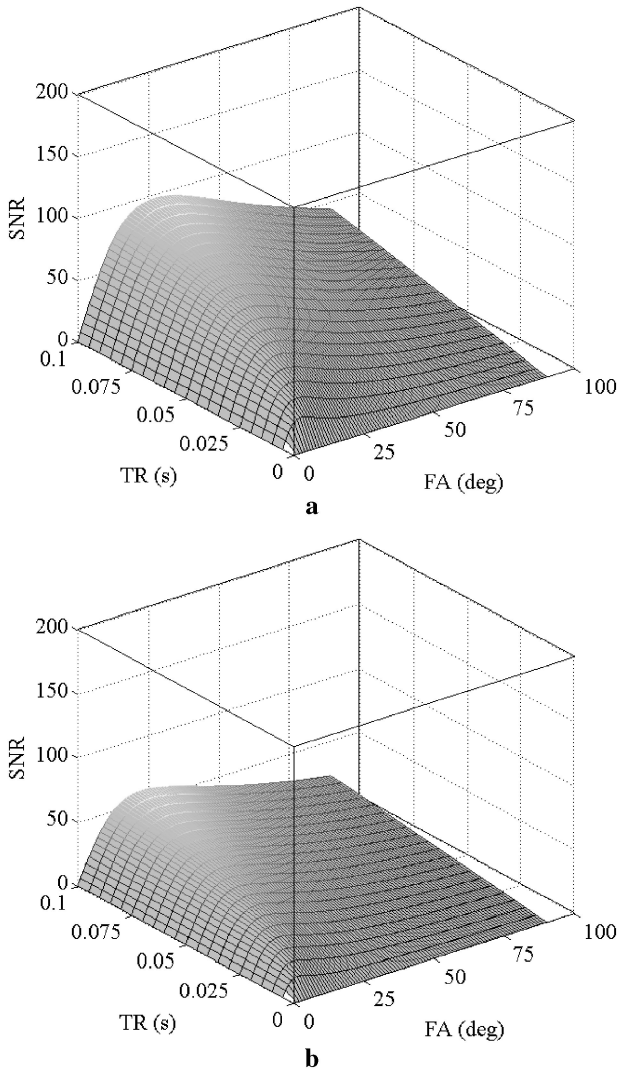

Fig. 6. Computer simulation: (**a**) Signal-to-noise ratio (SNR) of tumor (SNR_t) and (**b**) muscle (SNR_m) (tumor, 0.13 mM; muscle, 0.03 mM).

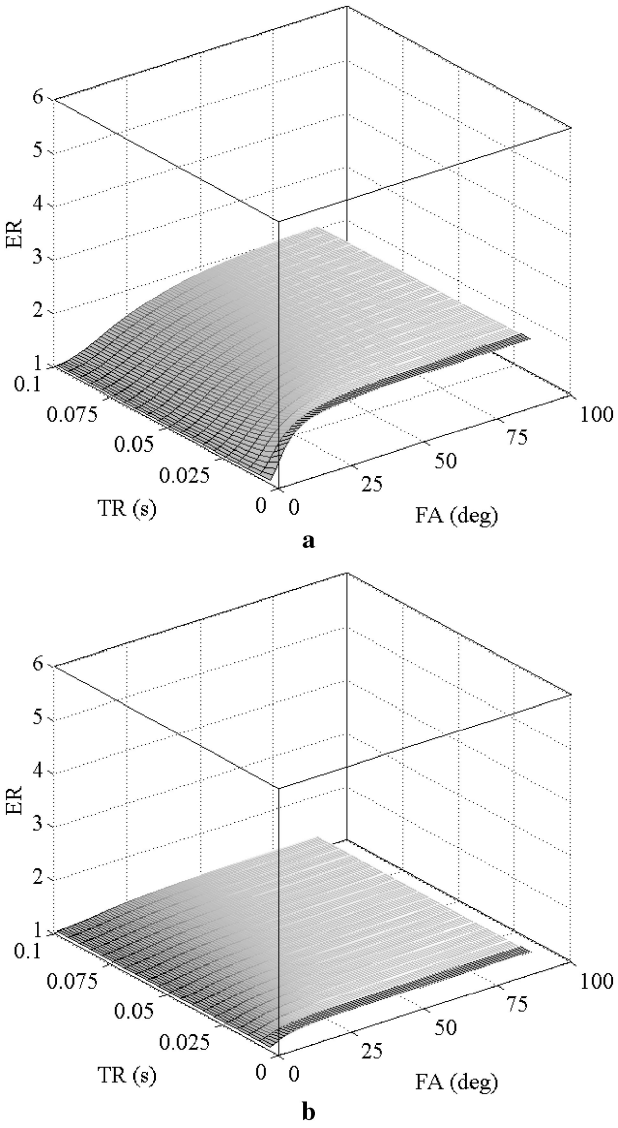

Fig. 7. Computer simulation: (**a**) Enhancement ratio (ER) of tumor (ER_t) and (**b**) muscle (ER_m) (tumor, 0.13 mM; muscle, 0.03 mM).

timal FA for the maximum CNR (CNR_{max}), and the optimal FA increased with TR as well. The optimal FA for CNR_{max} differed from that for SNR_{max}. SNR_{max}, ER_{max} and CNR_{max} for given TR and FA values were higher for a tumor with a higher concentration of gadobutrol (0.5 mM) than a tumor with a concentration of 0.13 mM gadobutrol (Figs. 8 and 9b).

Discussion

In this study, we investigated the impact of FA and TR on the ER_{max} of FSPGR T_1-weighted gadobutrol-enhanced MR imaging using an *in vivo* VX2 tumor model and computer simulation. In general, FA and TR are the 2 dominant factors that influence the MR signal intensity of SPGR T_1W images.

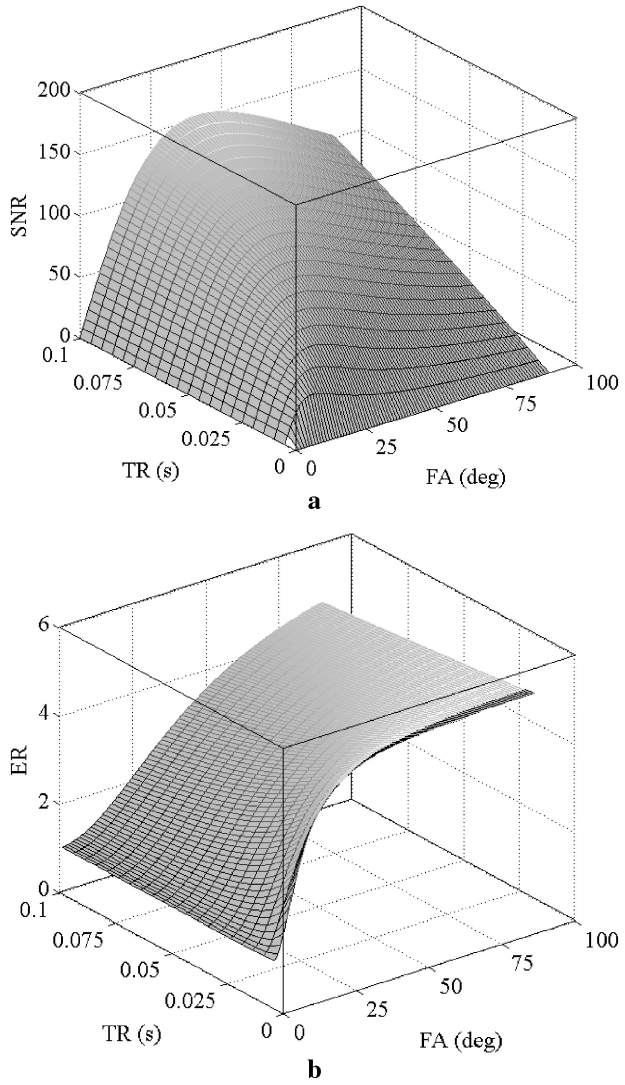

Fig. 8. Computer simulation: (**a**) Signal-to noise ratio of tumor (SNR_t) and (**b**) enhancement ratio of tumor (ER_t) (tumor, 0.5 mM; muscle, 0.03 mM).

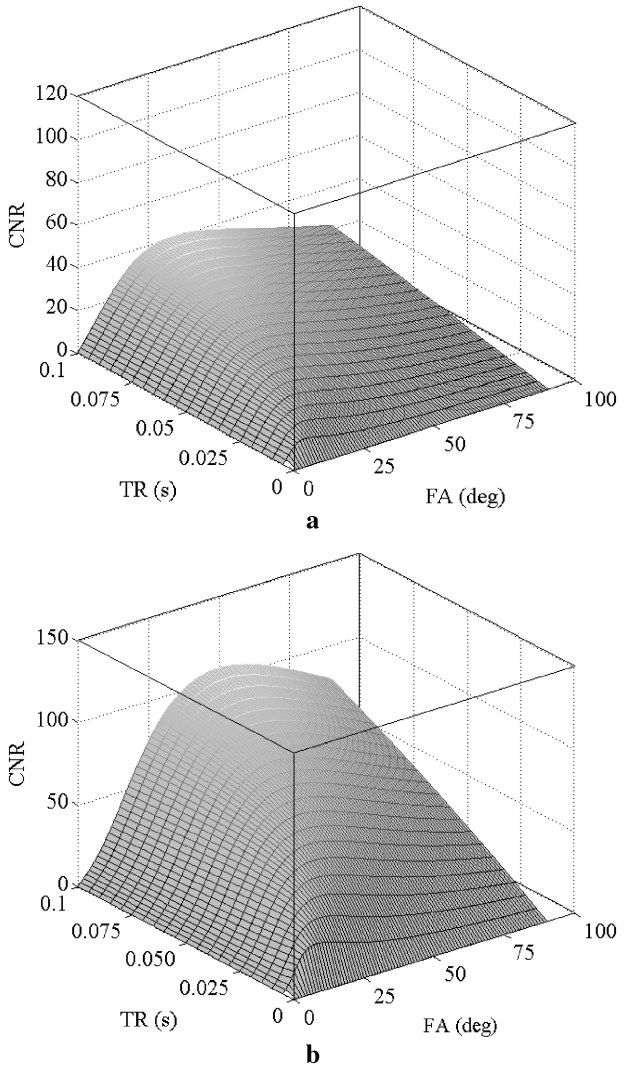

Fig. 9. Computer simulation: (**a**) Contrast-to-noise ratio of tumor (CNR_t) (tumor, 0.13 mM; muscle, 0.03 mM) and (**b**) CNR_t (tumor, 0.5 mM; muscle, 0.03 mM).

There were significant differences in ER_{max} and AUC_{100} of ER-time curves between the tumor and muscle. The ER_{max} value increased with FA (0°–90°) for a given TR for both computer simulation and single dosage gadobutrol-enhanced MR imaging. Furthermore, computer simulations demonstrated increased ER_{max} values with a higher concentration of gadobutrol (0.5 mM).

Computer simulation demonstrated that the ER value also increased with FA for a given TR in the closed interval [0, 90°] in tumors with a higher concentration of gadobutrol (0.5 mM). After injecting 0.1 mmol/kg gadobutrol, we obtained a C_{max} of gadobutrol of 0.13 mM in tumor. A higher injected dosage is expected to yield a higher concentration of gadobutrol in tumor. We assumed a gadobutol concentration of 0.5 mM in tumor with an injected dosage higher than 0.1 mmol/kg. From the result of simulation, we demonstrated the same tendency for monotonic increase of ER_{max} in the interval [0, 90°] for concentrations of both 0.13 and 0.5 mM. Therefore, it is expected that the tendency of optimal FA is similar for tumor concentration between 0.13 to 0.5 mM. The common routine dosages used clinically are 0.1 mmol/kg or sometimes 0.2 mmol/kg. A tumor concentration of 0.5 mM far exceeds clinically used double-dosage injection. Therefore, an estimated dosage of 0.5 mM is sufficient.

The scanning time of the T_1W SPGR pulse sequence is shorter, and the sequence has been widely used in DCE-MRI. The acquired MR signal intensity, shown in Eq. [7], depends on TR, TE, FA, T_1, T_2, and proton density. T_1, T_2, and proton density are the intrinsic properties of tissues and are independent of MR imaging pulse sequences. TE usually is set to the minimum value in the T_1W

SPGR pulse sequence, and the item $\frac{e^{-TE/T_2}}{e^{-TE/T_{20}}}$ is close to one. Therefore, the ER can be expressed approximately as:

$$ER = \left[\frac{\sin(FA)(1-e^{-TR/T_1})}{(1-\cos(FA)e^{-TR/T_1})}\right] \Big/ \left[\frac{\sin(FA)(1-e^{-TR/T_{10}})}{(1-\cos(FA)e^{-TR/T_{10}})}\right]. \quad [13]$$

Equation [13] is a strictly monotonic increasing function in the closed interval [0°, 90°], in which the highest ER value always occurs at an FA of 90°. This result agrees with those of *in vivo* study and computer simulation. The FA for the ER_{max} is always 90°, which may not be optimal for SNR_{max} or CNR_{max}.[24,25]

The ER value increases gradually with FA for longer TR and increases rapidly and plateaus for short TR. Consequently, ER values change little beyond some FA for a short TR. The 3-dimentional (3D) SPGR sequence is commonly used to cover a large volume of interest. A short TR and small FA are often used in 3D SPGR to shorten scan time. However, 2-dimensional (2D) SPGR is more suitable than 3D SPGR for fewer slices of interest. A shorter TR yields a low SNR with small coverage. Therefore, a longer TR is often used in 2D SPGR than that in 3D SPGR, which produces a more significant effect of FA on ER. In general, the choice of a larger FA will help increase ER in 2D SPGR, even in 3D SPGR.[26,27]

Angiogenesis generally produces greater blood flow in tumor than normal tissue. Use of a larger FA increases the effect of inflow, and the inflow effect could help to differentiate tumor from normal tissue. However, use of a larger FA increases the specific absorption rate (SAR), so the decision to use a larger FA to achieve a higher ER requires consideration of whether the SAR is within the permitted limitation. Nevertheless, the SAR of SPGR with FA 90° is less than that of fast spin echo (FSE) with FA 90° and 180°. Therefore, the SAR of SPGR with FA 90° is acceptable.

Compared to Gd-DTPA, gadobutrol has the benefit of less injection volume because of its high concentration formula. Images are sharper with gadobutrol than images obtained with Gd-DTPA in angiography.[21,28] Gadobutrol can be applied in tumor diagnosis as well. Its higher relaxivity than that of Gd-DTPA can produce higher ERs than those with Gd-DTPA.[29,30] In addition, gadobutrol has a good safety profile.[31] In the future, CAs with higher relaxivity will be helpful for increasing ER.

The computer simulation method of this study can be applied in humans with any kind of Gd-based contrast agent once the T_{10} and r_1 values of human organs are known. In this study, we used a conventional spin echo pulse sequence to measure T_{10} values because CSE can produce high quality images and take less scan time than conventional inversion recovery (CIR) pulse sequences. Though other fast imaging pulse sequences, such as Look-Locker or SPGR with various flip angles, can be used to obtain T_{10} in shorter scan time,[32,33] their image quality is worse than that with conventional spin echo. Many factors, including temperature, main field strength, and tissue type, may influence r_1 values, and acquisition of the actual r_1 *in vivo* is difficult. In this study, r_1 in the tissue is assumed to equal that in plasma *in vitro* at 37°C for 1.5T.[21] However, acquisition of an accurate r_1 *in vivo* remains a challenge. Nevertheless, even with such an approximation, the effect of FA and TR on ER can be estimated. The different assumption of r_1 values may change the values of SNR, CNR, AUC_{100}, and ER_{max} but will not change the behavior of the ER_{max} value versus the FA, i.e., the increased ER_{max} with FA for a given TR in the closed interval [0, 90°].

Conclusions

DCE-MRI is popular for diagnosing lesions and monitoring therapy. The ER_{max} and AUC_{100} obtained from ER-time curves could differentiate tumor from normal tissue. The maximum ER_{max} occurs at FA 90° according to *in vivo* study, computer simulation, and theoretical calculation. For short TR, the ER value was shown to increase rapidly with FA and then plateau. In conclusion, a higher FA, close to 90°, can obtain a higher ER_{max} for long TR in 2D SPGR or FSPGR, and a smaller FA, much less than 90°, can still reach appropriate ER values for short TR in 3D SPGR or FSPGR.

Acknowledgement

This work was supported by a grant from the National Science Council of Taiwan, R.O.C. (NSC 99-2221-E-214-008).

Appendix: Derivation of Eq. [6]

The enhancement ratio (ER) can be expressed as

$$ER = \left[\frac{(1-e^{-TR/T_1})}{(1-\cos(FA)e^{-TR/T_1})}e^{-TE/T_2^*}\right] \Big/ \left[\frac{(1-e^{-TR/T_{10}})}{(1-\cos(FA)e^{-TR/T_{10}})}e^{-TE/T_{20}^*}\right], \quad [A1]$$

where FA is the flip angle, TR is the repetition time, TE is the echo time, T_1 is the longitudinal relaxation time, T_2^* is the effective transverse relaxation time after CA injection, and T_{10} is the longitudinal relaxation time and T_{20}^* is the effective transverse relaxation time in the absence of CA. For T_1-weighted image,$(e^{-TE/T_2^*})/(e^{-TE/T_{20}^*}) \approx 1$, Eq. [A1] can be reduced to

$$ER = \left[\frac{(1-e^{-TR/T_1})}{(1-\cos(FA)e^{-TR/T_1})}\right] \Big/ \left[\frac{(1-e^{-TR/T_{10}})}{(1-\cos(FA)e^{-TR/T_{10}})}\right]. \quad [A2]$$

Substituting $B = \frac{(1-e^{-TR/T_{10}})}{(1-\cos(FA)e^{-TR/T_{10}})}$ into Eq. [A2] and rearranging it yields

$$[1 - B \cdot ER\cos(FA)]e^{-TR/T_1} = 1 - B \cdot ER \quad [A3]$$

The natural logarithm of

$$e^{-TR/T_1} = \frac{1 - B \cdot ER}{1 - B \cdot ER\cos(FA)} \quad [A4]$$

multiplied by $\frac{-1}{TR}$ on each side yields

$$\frac{1}{T_1} = \frac{-1}{TR}\ln\frac{1 - B \cdot ER}{1 - B \cdot ER\cos(FA)}. \quad [A5]$$

$$\frac{1}{T_1} = \frac{1}{T_{10}} + r_1 C, \quad [A6]$$

where C is the concentration of the contrast agent and r_1 is the longitudinal relaxivity.

Therefore, the concentration can be expressed as

$$C = \frac{-1}{r_1 TR}\ln\frac{1 - B \cdot ER}{1 - B \cdot ER\cos(FA)} - \frac{1}{r_1 T_{10}}. \quad [A7]$$

References

1. Chandarana H, Amarosa A, Huang WC, et al. High temporal resolution 3D gadolinium-enhanced dynamic MR imaging of renal tumors with pharmacokinetic modeling: preliminary observations. J Magn Reson Imaging 2013; 38:802–808.
2. McLaughlin R, Hylton N. MRI in breast cancer therapy monitoring. NMR Biomed 2011; 24:712–720.
3. Gollub MJ, Cao K, Gultekin DH, et al. Prognostic aspects of DCE-MRI in recurrent rectal cancer. Eur Radiol 2013; 23:3336–3344.
4. Takeuchi M, Matsuzaki K, Uehara H, Furumoto H, Harada M. Clear cell adenocarcinoma arising from clear cell adenofibroma of the ovary: value of DWI and DCE-MRI. Magn Reson Med Sci 2013; 12:305–308.
5. Jain R. Measurements of tumor vascular leakiness using DCE in brain tumors: clinical applications. NMR Biomed 2013; 26:1042–1049.
6. Vincensini D, Dedieu V, Eliat PA, et al. Magnetic resonance imaging measurements of vascular permeability and extracellular volume fraction of breast tumors by dynamic Gd-DTPA-enhanced relaxometry. Magn Reson Imaging 2007; 25:293–302.
7. Cao Y, Shen Z, Chenevert TL, Ewing JR. Estimate of vascular permeability and cerebral blood volume using Gd-DTPA contrast enhancement and dynamic T_2^*-weighted MRI. J Magn Reson Imaging 2006; 24: 288–296.
8. Durmus T, Vollnberg B, Schwenke C, et al. Dynamic contrast enhanced MRI of the prostate: comparison of gadobutrol and Gd-DTPA. Rofo 2013; 185:862–868.
9. Attenberger UI, Runge VM, Morelli JN, Williams J, Jackson CB, Michaely HJ. Evaluation of gadobutrol, a macrocyclic, nonionic gadolinium chelate in a brain glioma model: comparison with gadoterate meglumine and gadopentetate dimeglumine at 1.5 T, combined with an assessment of field strength dependence, specifically 1.5 versus 3 T. J Magn Reson Imaging 2010; 31:549–555.
10. Chang JM, Moon WK, Cha JH, Jung EJ, Cho N, Kim SJ. Dynamic contrast-enhanced magnetic resonance imaging evaluation of VX2 carcinoma in a rabbit model: comparison of 1.0-M gadobutrol and 0.5-M gadopentetate dimeglumine. Invest Radiol 2010; 45:655–661.
11. Priest AN, Gill AB, Kataoka M, et al. Dynamic contrast-enhanced MRI in ovarian cancer: initial experience at 3 tesla in primary and metastatic disease. Magn Reson Med 2010; 63:1044–1049.
12. Furukawa M, Parvathaneni U, Maravilla K, Richards TL, Anzai Y. Dynamic contrast-enhanced MR perfusion imaging of head and neck tumors at 3 Tesla. Head Neck 2013; 35:923–929.
13. Yuan Y, Kuai XP, Chen XS, Tao XF. Assessment of dynamic contrast-enhanced magnetic resonance imaging in the differentiation of malignant from benign orbital masses. Eur J Radiol 2013; 82:1506–1511.
14. Sasaki M, Shibata E, Kanbara Y, Ehara S. Enhancement effects and relaxivities of gadolinium-DTPA at 1.5 versus 3 Tesla: a phantom study. Magn Reson Med Sci 2005; 4:145–149.
15. Lei Z, Ma H, Xu N, Xi H. The evaluation of antiangiogenic treatment effects for implanted rabbit VX2 breast tumors using functional multi-slice spiral computed tomography (f-MSCT). Eur J Radiol 2011; 78:277–281.
16. Zheng LF, Li YJ, Wang H, et al. Combination of vascular endothelial growth factor antisense oligonucleotide therapy and radiotherapy increases the curative effects against maxillofacial VX2 tumors in rabbits. Eur J Radiol 2011; 78:272–276.
17. Shao H, Ni Y, Dai X, et al. Diffusion-weighted MR imaging allows monitoring the effect of combretastatin A4 phosphate on rabbit implanted VX2 tumor model: 12-Day dynamic results. Eur J Radiol 2012;

81:578–583.
18. Haacke EM, Brown RW, Thompson MR, Venkatesan R. Magnetic resonance imaging physical principles and sequence design. New York: John Wiley and Sons Inc, 1999; 128.
19. Pintaske J, Martirosian P, Graf H, et al. Relaxivity of gadopentetate dimeglumine (Magnevist), gadobutrol (Gadovist), and gadobenate dimeglumine (MultiHance) in human blood plasma at 0.2, 1.5, and 3 tesla. Invest Radiol 2006; 41:213–221.
20. Murase K. Generalized equation for describing the magnetization in spoiled gradient-echo imaging. Magn Reson Imaging 2011; 29:723–730.
21. Tuite DJ, Geoghegan T, McCauley G, Govender P, Browne RJ, Torreggiani WC. Three-dimensional gadolinium-enhanced magnetic resonance breath-hold FLASH imaging in the diagnosis and staging of renal cell carcinoma. Clin Radiol 2006; 61:23–30.
22. Stalder AF, Elverfeldt DV, Paul D, Hennig J, Markl M. Variable echo time imaging: signal characteristics of 1-M gadobutrol contrast agent at 1.5 and 3T. Magn Reson Med 2008; 59:113–123.
23. Woodward P, Freimarck R. MRI for technologists. New York: McGraw-Hill Inc, 1995; 146.
24. Schabel MC, Parker DL. Uncertainty and bias in contrast concentration measurements using spoiled gradient echo pulse sequences. Phys Med Biol 2008; 53:2345–2373.
25. De Naeyer D, Verhulst J, Ceelen W, Segers P, De Deene Y, Verdonck P. Flip angle optimization for dynamic contrast-enhanced MRI-studies with spoiled gradient echo pulse sequences. Phys Med Biol 2011; 56:5373–5395.
26. Haradome H, Grazioli L, Al manea K, et al. Gadoxetic acid disodium-enhanced hepatocyte phase MRI: can increasing the flip angle improve focal liver lesion detection? J Magn Reson Imaging 2012; 35: 132–139.
27. Bashir MR, Husarik DB, Ziemlewicz TJ, Gupta RT, Boll DT, Merkle EM. Liver MRI in the hepatocyte phase with gadolinium-EOB-DTPA: does increasing the flip angle improve conspicuity and detection rate of hypointense lesions? J Magn Reson Imaging 2012; 35:611–616.
28. Voth M, Haneder S, Huck K, Gutfleisch A, Schönberg SO, Michaely HJ. Peripheral magnetic resonance angiography with continuous table movement in combination with high spatial and temporal resolution time-resolved MRA with a total single dose (0.1 mmol/kg) of gadobutrol at 3.0 T. Invest Radiol 2009; 44:627–633.
29. Giesel FL, Mehndiratta A, Risse F, et al. Intraindividual comparison between gadopentetate dimeglumine and gadobutrol for magnetic resonance perfusion in normal brain and intracranial tumors at 3 Tesla. Acta Radiol 2009; 50:521–530.
30. Morelli JN, Runge VM, Vu L, Loynachan AT, Attenberger UI. Evaluation of gadodiamide versus gadobutrol for contrast-enhanced MR imaging in a rat brain glioma model at 1.5 and 3 T. Invest Radiol 2010; 45:810–818.
31. Forsting M, Palkowitsch P. Prevalence of acute adverse reactions to gadobutrol–a highly concentrated macrocyclic gadolinium chelate: review of 14,299 patients from observational trials. Eur J Radiol 2010; 74:e186–e192.
32. Amano Y, Tachi M, Kumita S. Three-dimensional Look-Locker MRI for evaluation of postcontrast myocardial and blood T_1 values: comparison with two-dimensional Look-Locker and late gadolinium enhancement MRI. Acta Radiol 2013; 54:8–13.
33. Trzasko JD, Mostardi PM, Riederer SJ, Manduca A. Estimating T_1 from multichannel variable flip angle SPGR sequences. Magn Reson Med 2013; 69:1787–1794.